Rev. LatinAm. Metal. Mat.

Artículo Regular

www.rlmm.org

COEXISTENCE OF SUPERPARAMAGNETIC AND FERROMAGNETIC COMPONENTS IN $(CuGa)_{1-x}Fe_xSe_{2-x}$ SOLID SOLUTIONS WITH x=0.1, 1/3 and 1/2

P. Grima-Gallardo[1,2], L. Nieves[1], M. Soto[1], M. Quintero[1], H. Cabrera[3,4], I. Zumeta-Dubé[5], A. Rodríguez[5], J. A. Aitken[6] and D.P. Rai[7]*

1: Centro de Estudios en Semiconductores (CES). Dpto. Física. Fac. Ciencias. Universidad de Los Andes (ULA). Mérida. Venezuela. 2: Centro Nacional de Tecnología Óptica (CNTO). Mérida. Venezuela. 3: International Centre for Theoretical Physics (ICTP), Trieste, Italy. 4: Centro Multidisciplinario de Ciencias, Instituto Venezolano de Investigaciones Científicas (IVIC), Mérida, Venezuela. 5: Centro de Investigación en Ciencia Aplicada y Tecnología Avanzada, Unidad Legaria, Instituto Politécnico Nacional, México. 6: Department of Chemistry and Biochemistry, Duquesne University, Pittsburgh, USA. 7. Department of Physics, Pachhunga University College, Aizawl, India-796001.

**e-mail: peg@ula.ve*

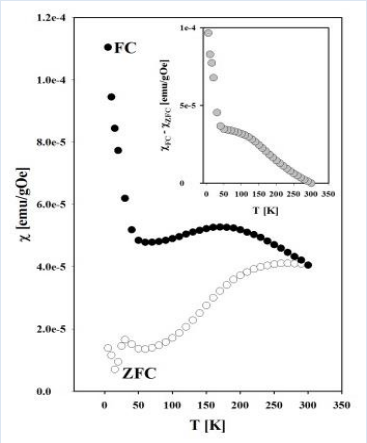

ABSTRACT

The magnetic behavior of $(CuGa)_{1-x}Fe_xSe_{2-x}$ solid solutions with compositions x=0.1, 1/3 and 1/2 has been investigated using SQUID techniques. DC magnetic susceptibility was measured in the temperature range 2 < T < 300K using Zero Field Cooling (ZFC) – Field Cooling (FC) protocol. It has been observed that the experimental curves can be analyzed as the sum of two magnetic components, one superparamagnetic and the other one ferromagnetic. The ferromagnetic component persist up to temperatures higher than room temperature making this report the first observation of room temperature ferromagnetism in $A^IB^{III}C^{VI}_2$ compounds doped (or alloyed) with transition metals.

Keywords: $CuGaSe_2$, FeSe, magnetic susceptibility, ferromagnetism, superparamagnetism.

COEXISTENCIA DE COMPONENTES FERROMAGNÉTICA Y SUPERPARAMAGNÉTICA EN SOLUCIONES SÓLIDAS $(CUGA)_{1-X}FE_XSE_{2-X}$ CON X=0.1, 1/3 Y 1/2

RESUMEN

El comportamiento magnético de las soluciones solidas $(CuGa)_{1-x}Fe_xSe_{2-x}$ con composiciones x=0.1, 1/3 y 1/2 fue investigado por medio de la técnica de SQUID. Las susceptibilidades DC fueron medidas en el rango de temperatura 2 < T < 300K usando el protocolo Enfriamiento a Campo Zero (ECZ) – Enfriamiento con Campo (EC). Se observó que las curvas experimentales podían ser analizadas como la suma de dos componentes magnéticas, una superparamagnética y otra ferromagnética. La componente ferromagnética persiste a temperaturas por arriba de la temperatura ambiente siendo este reporte la primera observación de ferromagnetismo a temperatura ambiente en compuestos $A^IB^{III}C^{VI}_2$ dopados (o aleados) con metales de transición.

Palabras clave: $CuGaSe_2$, FeSe, susceptibilidad magnética, ferromagnetismo, superparamagnetismo.

Recibido: 26-07-2017 ; **Revisado:** 31-10-2017

Aceptado: 08-11-2017 ; **Publicado:** 16-03-2018

pISSN: 0255-6952 | eISSN: 2244-7113

Rev. LatinAm. Metal. Mat. 2018; **38** (2): 128-135

1. INTRODUCTION

Conventional electronic devices rely on the transport of electrical charge carriers in a semiconductor. Spintronics exploits the spin of the electron rather than its charge to create a new generation of devices, which will be smaller, more versatile and more robust than those currently making up silicon chips and circuit elements [1-2]. Due to these great advantages, intensive attention has been paid to semiconductor based ferromagnetic (FM) materials, including $A^{I}B^{III}C^{VI}_2$ and $A^{II}B^{IV}C^{V}_2$ chalcopyrite semiconductors. For $A^{II}B^{IV}C^{V}_2$, ferromagnetism above room temperature was reported in several $A^{II}B^{IV}C^{V}_2$: Mn alloys (see Table I) but there are no reports of such behavior in analogous $A^{I}B^{III}C^{VI}_2$: Mn alloys.

Ferromagnetism in $A^{II}B^{IV}C^{V}_2$: Mn alloys is thought to arise from the interaction of holes (created by substitution of a IV-element by Mn^{2+}) with the local moment of the *d* electrons of Mn [11, 12]; however it is sometimes argued that it can be also produced by the presence of magnetic secondary phases such as MnP and MnAs [13-16]. Kochura *et al* (2013), in samples prepared by solid state reaction under the condition of fast cooling, found three types of magnetic species: a) the substitutional Mn ions making Mn complexes (especially dimers), b) the MnAs micro-precipitates and c) nanosize precipitates (MnAs clusters with mean diameter of 3nm) [13]. Although the origin of room temperature ferromagnetism in these compounds is until now under investigation, it seems well established that the magnetic behavior of these alloys is composition dependent: at low values of x, the alloys show a typical paramagnetic behavior (or also superparamagnetic) [6, 8] until a critical x_c value is reached, for which a paramagnetic→ferromagnetic transition occurs. It is worth to note here, by inspection of Table I, that T_c values are approximately the same for all the $A^{II}_{1-x}Mn_xB^{IV}C^{V}_2$ alloys suggesting that this transition is related to with Mn-based secondary phases more than substitution in the ternary matrix.

Table I. $A^{II}B^{IV}C^{V}_2$: Mn alloys showing room temperature ferromagnetism.

Alloys	Magnetic element composition	Synthesis method	T_c [K]	Reference
$Cd_{1-x}Mn_xGeP_2$	x=0.2	SSR	300	[3]
$Zn_{1-x}Mn_xGeP_2$	x=0.056	SSR	312	[4]
$(ZnGe)_{1-x}Mn_xAs_2$ $(ZnSn)_{1-x}Mn_xAs_2$	x=5 mass % x=1.2 mass %	BM	333 329	[5]
$(CdGe)_{1-x}Mn_xAs_2$	x=6 mass %	SSR	355	[6]
$(ZnGe)_{1-x}Mn_xAs_2$	x=3.5 mass %	SSR	367	[7]
$(ZnSi)_{1-x}Mn_xAs_2$	x=1 mass % x=2 mass %	SSR	325 337	[8]
$Zn_{1-x}Mn_xGeAs_2$	x=0.078	SSR	320	[9]
$(Zn_{0.9}Cd_{0.1})_{1-x}Mn_xGeAs_2$	x=1.13 mass % x=2.65 mass %	SSR	349 351	[10]

T_c: critical temperature (magnetic transition temperature from paramagnetic to ferromagnetic).
SSR: Solid State Reaction; BM: Bridgman Method.

Table II. Magnetic behavior $A^{II}B^{IV}C^{V}_2$: Mn alloys.

Compound	Magnetic element composition	Synthesis method	Magnetic behavior	Ref.
$Cu_{1-x}Mn_xInTe_2$	x=0.03 and 0.06 x=0.09 and 0.12	SSR	PM AFM	[17]
$(CuIn)_{1-x}Mn_{2x}Te_2$	$0.010 \leq x \leq 0.101$	BM	SG	[18]
$CuIn_{1-x}Mn_xS_{2-\delta}$ $Cu_{x/2}In_{x/2}Mn_xS_2$	x=0, 0.05, 0.1 and 0.2 x=0.1	SSR	AFM	[19]
$CuIn_{1-x}Mn_xS_2$ $Cu_{1-x}Mn_xInS_2$	x = 0 – 0.2 x = 0 – 0.1	SSR	PM	[20]
$Cu_{0.95-x}Mn_{0.05}InSe_2$	x = 0-0.20	SSR	PM	[21]
$CuIn_{1-x}Mn_xSe_2$ $Cu_{1-y}In_{1-y}Mn_{2y}Se_2$	x = 0.0125-0.2 2y = 0.0125 – 0.6	SSR	PM	[22]
$Cu_{x/2}Ga_{x/2}Mn_xTe_2$	x=0.2	SSR	SPM	[20]
$Cu_{1-x}Mn_{2x}InS_2$ $Cu_{1-x}Mn_{2x}AlS_2$	x=0.03 x=0.01	SSR	PM + weak FM	[21]
$CuGa_{1-x}Mn_xTe_2$ $Cu_{1-x}Ga_{1-x}Mn_{2x}Te_2$	x=0.004, 0.008, 0.010 and 0.012	SSR	SPM	[22]

SSR: Solid State Reaction; BM: Bridgman Method; PM: Paramagnetic; AFM: Antiferromagnetic; Spin Glass; SPM: Superparamagnetic; FM: Ferromagnetic

Table III. $A^{II}B^{IV}C^{V}_2$ compounds doped (or alloyed) with a TM different than Mn.

Compound	Magnetic element composition	Synthesis method	Magnetic behavior	Ref.
$CuIn_{1-x}Fe_xS_2$	x=0.1	SSR	AF	[19]
$(CuIn)_{1-x}Fe_xTe_{2-x}$ $(CuGa)_{1-x}Fe_xTe_{2-x}$	x=0.5	SSR	SPM	[26]
$(CuIn)_{1-x}Fe_xSe_{2-x}$	x=0.5	SSR	SPM	[27]
$(CuAl)_{1-x}Cr_xS_{2-x}$	x=0.1 and 0.2 x=0.33	SSR	AFM	[28] [29]
$(CuIn)_{1-x}Co_xTe_{2-x}$ $(CuIn)_{1-x}Ni_xTe_{2-x}$	x=0.67	SSR	SPM DM + weak FM	[30]
$(CuIn)_{1-x}Ta_xTe_{2-x}$	x=0.25	SSR	SPM	[31]
$(CuIn)_{1-x}Ta_xSe_{2-x}$ $(CuIn)_{1-x}Ta_xTe_{2-x}$	x=0.25 x=2/3	SSR	SG FM (T_c~50K)	[32]

SSR: Solid State Reaction; DIA: Diamagnetic; PM: Paramagnetic; AFM: Antiferromagnetic; Spin Glass; SPM: Superparamagnetic; FM: Ferromagnetic.

The experimental reports of $A^{I}B^{III}C^{VI}_2$: Mn alloys are summarized in Table II. No room temperature ferromagnetism has been reported for these alloys until now. For low values of x, paramagnetic (or superparamagnetic) behavior is observed as in $A^{II}B^{IV}C^{V}_2$: Mn alloys, but for higher values of x the

magnetic transition goes from paramagnetic to antiferromagnetic or paramagnetic to spinglass magnetic states. In the case of $Cu_{1-x}Mn_{2x}InS_2$ and $Cu_{1-x}Mn_{2x}AlS_2$ alloys heterogeneous behavior was observed where a paramagnetic state coexists with a weak ferromagnetic component [21]. For $CuGaTe_2$: Mn alloys, superparamagnetic behavior had been reported [20, 22]. Whereas $A^{II}B^{IV}C^{V}_2$ compounds have been investigated almost exclusively alloyed with Mn, $A^{I}B^{III}C^{VI}_2$ materials have been alloyed with other transition metals (TMs) such as Fe, Cr, Co, Ni and Ta; the published work up to now is given in Table III. As in the case of alloys with Mn, a variety of magnetic behaviors are observed: antiferromagnetic, superparamagnetic, spinglass, coexistence of magnetic components but also a report of ferromagnetism at low temperature (T_c~50K) in $(CuIn)_{1-x}Ta_xTe_{2-x}$ at x=2/3.

It is interesting to compare experimental results with those obtained by theoretical calculations. Katamani *et al* (2003) [33, 34] using KKR-CPA-LDA method predict that ferromagnetic states are stable in $(Cd_{1-x}V_x)GeP_2$ and $(Cd_{1-x}Cr_x)GeP_2$, alloys whereas $(Cd_{1-x}Mn_x)GeP_2$, $(Cd_{1-x}Fe_x)GeP_2$ and $(Cd_{1-x}Co_x)GeP_2$ alloys must show spinglass-like ground states (calculations were made using x=0.1); Ti and Ni substitutions in $CdGeP_2$ could not have a net magnetic moment (the same are applicable to $ZnGeP_2$ and $CdSiAs_2$). On the other hand, the ferromagnetic state was found to be stable in $AgGaS_2$ ($CuAlS_2$) doped with Ti, V, Cr and Mn, whereas doping with Fe, Co and Ni must stabilizes a spinglass-like state. The work of Zhao *et al* (2004) [35], using first principle calculations, coincides with Katamani and predicts that Mn doping at the III site in $A^{I}B^{III}C^{VI}_2$ compounds provides holes that must stabilize ferromagnetic coupling between Mn ions. The prediction of both works (Katamani and Zhao) is contradictory that which has been observed experimentally! The reason for the discrepancies between theoretical expectations and experimental results is not clear until now. It has been suggested, that stabilization of ferromagnetism is due to the interaction of holes with Mn magnetic moments induced by: a) intrinsic defects [36, 37]; b) non-uniform spatial distribution of carriers and/or and magnetic ions [38]; or c) nanoscale phase separation driven either by randomness in the carrier and spin subsystems or by limited solubility of transition metals in the host semiconductor, which leads to spinodal decomposition into regions with a small and a large concentration of the magnetic constituents [38]. It is evident that additional experimental work, in greater variety of systems and with larger concentration of the transition metal dopant, is necessary.

In this work, we have studied the magnetic behavior of the $(CuGa)_{1-x}Fe_xSe_{2-x}$ alloy system with x= 0.1, 1/3 and 1/2. Previously, we reported the phase diagram of this alloy system in the composition interval $0 \leq x \leq 0.5$ [39], finding that up to composition x=0.333 the alloys are single phase and in the composition interval $0.333 < x < 0.5$ the alloys show traces of two secondary phases identified as α-FeSe [40] and Fe_7Se_8 [41].

2. EXPERIMENTAL PROCEDURE

The preparation of the samples, X-ray diffraction (XRD) measurements, differential thermal analysis (DTA) and the T-x phase diagram of the $(CuGaSe_2)_{1-x}(FeSe)_x$ alloy system for $0 \leq x \leq 0.5$ have been reported previously [39]. DC magnetic susceptibility and magnetization (H,T) measurements were performed on a Quantum Design SQUID magnetometer, equipped with a superconducting magnet able to produce fields up to 5 T. The samples in the form of powder were compacted with a piece of cotton inside the sample holder in order to prevent any movement. Zero-field-cooling and field cooling (ZFC-FC) measurements were carried out in the temperature range of 2–300 K. The ZFC protocol consists of cooling the sample from high temperature, to the lowest measuring temperature in zero magnetic field. Then a static magnetic field of 0.5 kOe is applied and the magnetization is measured during warm up. The FC protocol consists of cooling the sample in a small DC field and measuring the magnetization during cooling without removal of the field.

3. RESULTS AND DISCUSSION

DC magnetic susceptibility (χ) as a function of temperature (T) for samples x=0.1, 1/3 and 1/2 are show in figure 1.

The magnetic behavior of ZFC and FC curves for composition x=0.1 is typical of a paramagnetic-like component. However, the observed hysteresis is indicative of the formation of some magnetic clusters that coexist with the predominant paramagnetic-like component; at the lower temperature, for a virgin sample, the clusters must be blocked and the large

magnetization value is completely due to the paramagnetic-like component. The hysteresis, as a function of temperature (given in the insert as the difference between χ_{ZFC} and χ_{FC} curves) decreases abruptly in the interval 2K<T<50K, shows a plateau in the interval 50K<T<100K, and then decreases linearly in the interval 100K<T<300K, due to the gradual unblocking of the magnetic clusters at different magnetic regimes characteristic of systems where magnetic clusters have a size distribution.

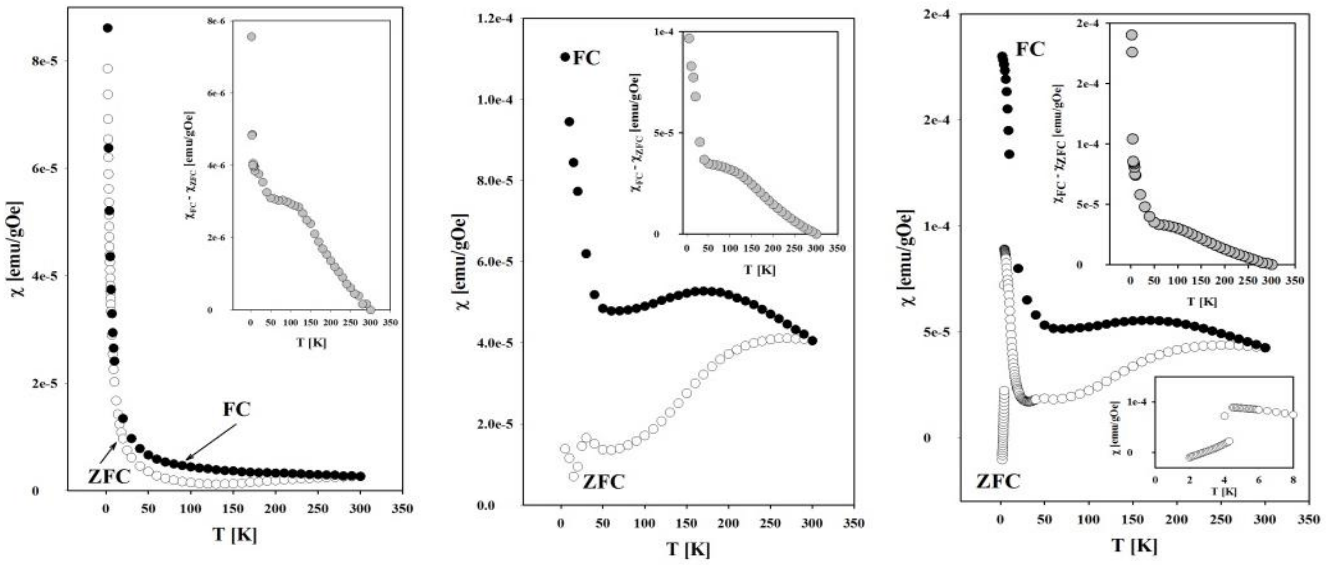

Figure 1. χ vs T for samples (from left to right) x= 0.1, 1/3 and 1/2. ZFC: white circles; FC: black circles. In the inserts, at the top, the difference between FC and ZFC curves (hysteresis) are also displayed. For sample x=1/2 amplification at the lowest temperature is also showed.

For sample with composition x=1/3, the ZFC curve show their minimum value at the lower temperature as it is usual in magnetic systems conformed by blocked magnetic clusters (the observed dispersion of the points is probably due to the presence of little traces of a secondary phase which has not previously observed in the diffraction pattern). When the temperature increases, the clusters gradually unblock suggesting a system with a distribution of clusters sizes as before, for sample x=0.1. The plateau at 250-300K is indicative that the majority of the clusters are unblocked. The magnetic behavior of the FC curve suggests the presence of two magnetic components, one ferromagnetic that dominates at high temperature and another paramagnetic-like that dominates at low temperature. The difference between FC and ZFC curves (insert) repeats the behavior observed for composition x=0.1.

For composition x=1/2, the ZFC curve at the lowest temperature shows a diamagnetic character (negative magnetization) and a step transition to positive magnetization at around 4K (see insert at the bottom). This behavior is typical of a superconductor and it is probably due to the presence of the α-FeSe secondary phase observed in the diffraction pattern for this composition for which an analogous transition has been reported [42]. For higher temperatures the contribution of the α-FeSe secondary phase disappears at the observed magnetization is due to the unblocking clusters as in the case of composition x=1/3.

In Figure 2, we analyze the magnetic susceptibility curves as a linear combination of two magnetic components, where *z* is the relative portion of each of them:

$$\chi_{Total} = z\chi_{FM} + (1-z)\chi_{PM} \quad (1)$$

The paramagnetic contribution has been written as:

$$\chi_{PM} = \chi_0 L(x) \quad (2)$$

Where $L(x) = \left({}^{cth(\mu_c H)}/_{kT} - {}^{kT}/_{\mu H}\right)$ is the Langevin function [43], μ_c is the mean magnetic moment of the clusters, H is the applied magnetic field, k is the Boltzmann constant and T is the absolute temperature. First, we are fitted the experimental curve (black circles) with equation (2). Then, the ferromagnetic component (blue line) is obtained from the difference between the experimental curve and the fitted paramagnetic-like component (red line). The sum of the ferromagnetic and the paramagnetic-like components is given by continuous black line.

In Figure 3, the *z* values for each component as a function of temperature are showed.

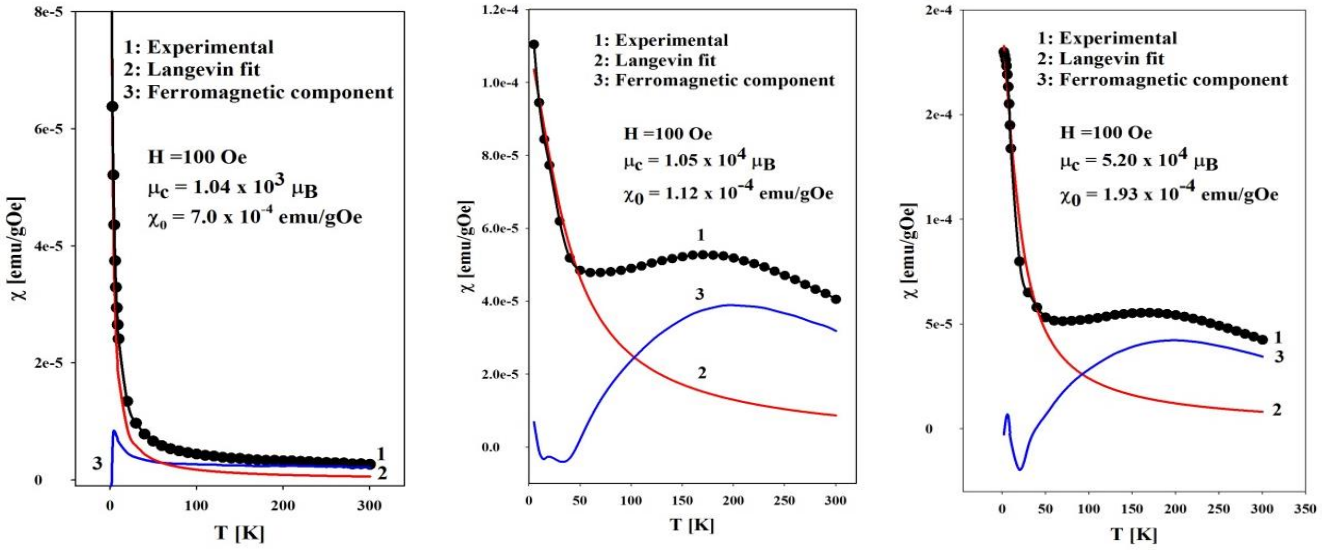

Figure 2. Fitting of the experimental FC curves considering the existence of two coexisting magnetic components. From left to right, x=0.1, 1/3 a 1/2. Black circles: experimental; red line: paramagnetic-like component; blue line: ferromagnetic-like component; and black line: paramagnetic-like + ferromagnetic. The fitting parameters μ_c and χ_0 are indicated for each curve, together with the applied magnetic field value.

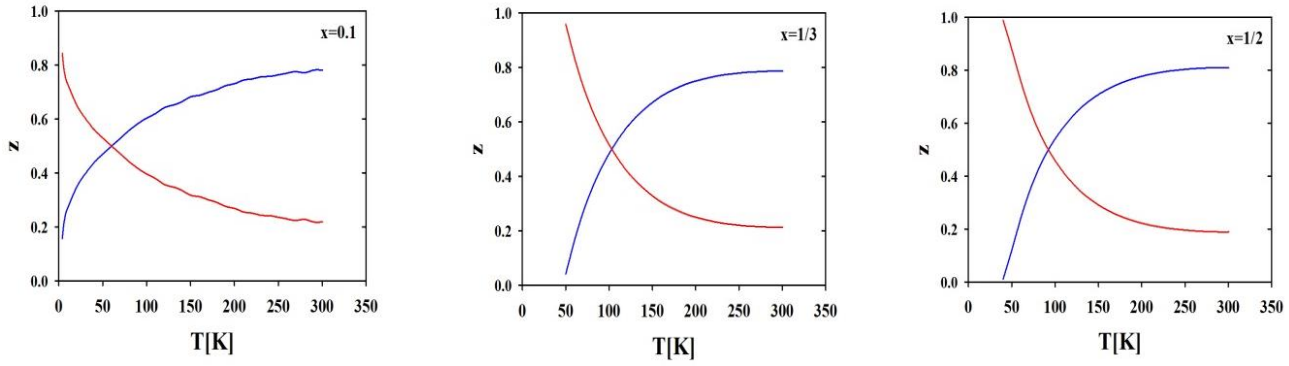

Figure 3. *z* Vs T for the compositions x=0.1, 1/3 and 1/2. Red line: paramagnetic-like component; blue line: ferromagnetic component.

From the fit, the mean magnetic moment was obtained and in Figure 4, these values are displayed as a function of composition.

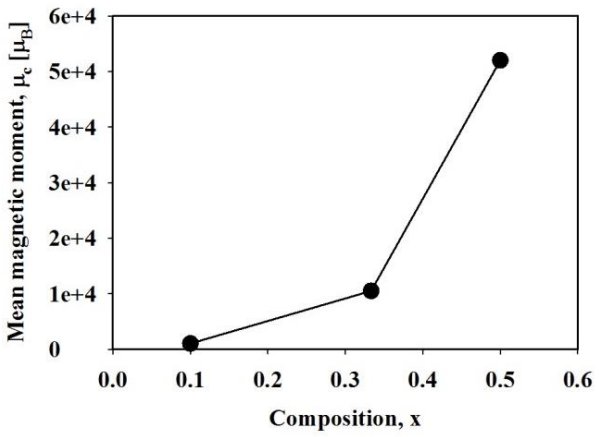

Figure 4. Mean magnetic moment (μ_c) versus composition.

The mean magnetic moments are equivalent to 176, 1780 and 8814 Fe^{3+} ions ($5.9\mu_B$/ion) for compositions x=0.1, 1/3 and 1/2, respectively. This calculation implies that the paramagnetic-like phase is in reality superparamagnetic composed by clusters which size increases exponentially with composition. From figure 3, it is worth to note that, at room temperature, the total magnetic component is given by 80% ferromagnetic and 20% superparamagnetic, for all the samples.

4. CONCLUSIONS

The analysis of the experimental curves of the magnetic susceptibility permitted us to conclude the presence of two magnetic components: one superparamagnetic (it has the behavior of a normal paramagnetic, with one notable exception, the mean magnetic moment increases very fast with composition up to 5.2×10^4 μ_B for x=1/2, indicating the presence of magnetic clusters) and another ferromagnetic with a critical temperature $T_c > 300K$, making this the first observation of room temperature ferromagnetism in $A^IB^{III}C^{VI}_2$ compounds doped (or alloyed) with TM.

The high value of the mean magnetic moment and the fact that at room temperature the magnetism of the sample is 80% ferromagnetic, suggest that these alloys could be used as magnetic devices in spintronics applications.

5. ACKNOWLEDGEMENT

P.G-G wants to thank to CDCHTA-ULA grant code C-1885-14-05-B and Fondo Nacional de Ciencia, Tecnología e Innovación (FONACIT) project number 2011001341. I.Z-D acknowledges postdoctoral fellow from CONACyT project number 174247 (Desarrollo de Materiales para Tecnologías de Energías Renovables).

6. REFERENCES

[1]. Spintronics (Semiconductors and Semimetals, Vol. 82). Edited by Dielt, T, Awschalom D.D., Kaminska M. and Ohno H. Academic Press, Elsevier, 2008.

[2]. Dielt, T, Ohno H., Matsukura F, Cibert J and Ferrand D. Science 2000; 287: 1019.

[3]. Medvedkin G.A., Ishibashi T., Nishi T., Hayata K., Hasewaga Y., and Sato K., Jpn. J.Appl. Phys. 2000; 39: L949-L951.

[4]. Cho S., Choi S., Cha G.-B., Hong S.C., Kim Y., Zhao Y.-J., Preeman A.J., Ketterson J.B., Kim B.J., and Choi B.-C., Phys. Rev. Lett. 2002; 88: 257203.

[5]. Cho S., Cho J., Hong S.C. and Cho S. J. Korean Phys. Soc. 2003; 42: S739-S741

[6]. Demin R.V., Koroleva L.I., Marenkin S.F., Mikhailov S., Aminov T., Szymczakc H., Szymczakc R., and Baran M., J. Magn. Magn. Mater. 2005; 290/291: 1379.

[7]. Koroleva L.I., Pavlov V.Yu., ZashchirinskiĬ D.M., Marenkin S.F., Varnavskiĭ S.A., Szymczakc R., Dobrovolśkiĭ V., and Killanskiĭ L., Phys. Solid State 2007; 49: 2121.

[8]. Koroleva L.I., ZashchirinskiĬ D.M., Khapaeva T.M., Marenkin S.F., Fedorchenko I.V., Szymczakc R., Krzumanska B., Dobrovolśkiĭ V., and Killanskiĭ L. Phys. Solid State 2009; 51(2): 303-308.

[9]. Kilanski L., Gorska M., Domukhovski V., Dobrowolski W., Anderson J.R., Rotundu C.R., Varniavskii S.A. and Marenkin S.F. Acta Physica Polonica 2008; 114: 1151-1157.

[10]. Kochura A.V., Laiho R., Lashkul A., Lähderanta E., Shakhov M.S., Zakharov I.S., Marenkin S.F., Molchanov A.V., Mikhailov S.G. and Jurev G.S. J. Phys. Cond. Matter. 2008; 20: 1-5.

[11]. Zhao Y-J and Zunger A. Phys. Rev. B 2004; 69: 104422.

[12]. Zhao Y-J and Zunger A. Phys. Rev. B 2004; 69: 075208.

[13]. Kochura A.V., Ivanenko S.V., Lashkul A., Kochura E.P., Marenkin S.F., Fedorchenko I.V., Kuzmenko A.P. and Lahderanta E. J. Nano and Electronic Physics 2013; 5: 04013-04016.

[14]. Kilanski L., Dobrowolski W., Szymczak R., Dynowska E., Wójcik M., Romcevic N., Fedorchenko I.V. and Marenkin S.F. Science of

Sintering 2014; 46: 271-281.

[15]. Aitken, J.A., Tsoi G.M., Wenger L.E., Brock S.L. Chem. Mater. 2007; 83:1809.

[16]. Hwang T., Ohno H., Matsukura F. Phys. Rev. B 2001; 63:195205.

[17]. Lin L-J, Tabatabaie N., Wernick J.H., Hull G.W. and Meagher B. J. Elect. Mater. 1988; 17: 321-324.

[18]. Shand P.M., Polstra P.A., Miotkowski I. and Crooker B.C. J. Appl. Phys. 1994; 75(10): 5731-5733.

[19]. Tsuji N., Kitazawa H. and Kido G. Phys. Stat. Sol. (a) 2002; 189(3): 951-954.

[20]. Yao, J., Rudyk, B. W., Brunetta, C. D., Knorr, K. B., Figore, H. A., Mar, A. and Aitken, J. A. Mat. Chem. Phys. 2012; 136: 415-423.

[21]. Yao, J., Brunetta, C. D. and Aitken, J. A. J. Phys.: Condens. Matter. 2012; 24: 086006.

[22]. Yao, J., Kline, C. N., Gu, H., Yan, M. and Aitken, J. A. J. Solid State Chem. 2009; 182: 2579-2586.

[23]. Demin R.V., Koroleva L.I., Marenkin S.F., Novotortsev V.M., Trukhan B.M., Varnavskiib S.A., Aminov T.G., Shabuninab G.G., Szymczakc R., and Baranc M., Heterogeneous magnetic state in Mn-doped CdGeP2 and CuGaTe2, Proc. 3rd Moscow Int. Symp. on Magnetism (2005).

[24]. Schorr S., Hoehne R., Spemann D., Doering Th. And Korzun B.V. Phys. Stat. Sol. (a) 2006; 203(11):2783-2787.

[25]. Novotortsev V.M., Shabuninab G.G., Koroleva L.I., Aminov T.G., Demin R.V. and Boichuk S.V. Inor. Mater. 2007; 43(1): 12-17.

[26]. Grima-Gallardo P., Alvarado F., Muñoz M., Durán S., Quintero M., Nieves L., Quintero E., Tovar R., Morocoima M. and Ramos M.A. Phys. Stat. Sol. A 2012:1-3.

[27]. Torres-Cuenza S., Grima-Gallardo P., Muñoz M., Durán S., Quintero M., Nieves L. and Tovar R. Acta Científica Venezolana 2015; 66(1):56-59.

[28]. Villarreal M.A., Grima-Gallardo P., Quintero M., Moreno E., Calderón E., Delgado G.E., Silva P. and Villegas J. Acta Científica Venezolana 2015; 66(3):145-151.

[29]. Villarreal M.A., Grima-Gallardo P., Quintero M., Moreno E., Delgado G.E., Fernández J., Silva P. and Villegas J. Rev. LatinAm. Metal. Mat. 2012; 32(2):292-298

[30]. Grima-Gallardo P., Soto M., Izarra O., Nieves L., Quintero M., Delgado G.E., Cabrera H., Zumeta-Dubé I., Rodríguez A., Glenn J.R., Aitken J.A. Rev. LatinAm. Metal. Mat. 2017; 37(2):83-92.

[31]. Grima-Gallardo P., Izarra O., Peña R., Muñoz M., Durán S., Quintero M., Quintero E. and Romero H. Rev. Cuba Fis. 2015; 32(1);1-6.

[32]. Grima-Gallardo P., Calderón E., Muños-Pinto M., Durán-Piña S., Quintero M., Quintero E., Morocoima M., Delgado G.E., Romero H., Briceño J.M. and Fernández J. Phys. Stat. Sol. (a) 2008; 205(7); 1552-1559.

[33]. Katamani T and Akai H. J. Superconductivity 2003; 16: 95-97.

[34]. Katamani T and Akai H.J. Materials Science in Semiconductor Processing 2003; 6: 389-391.

[35]. Zhao Y-Jun and Zunger A. Phys. Rev. B 2004; 69: 104422.

[36]. Mahadevan P. and Zunger A. Phys. Rev. Lett. 2001; 88:047205.

[37]. Akai H. Phys. Rev. Lett. 1998; 81: 3002.

[38]. Dietl D. J. Phys.: Condens. Matter. 2007; 19: 165204.

[39]. Soto M., Grima-Gallardo P., Quintero M., Salas M., Muñoz M.m Durán S., Nieves L., Moreno E., Ramos M.A. and Briceño J.M. Rev. LatinAm. Metal. Mat. 2013; 33(2): 200-205.

[40]. Hägg G. and Kindström A.L. Z. Phys. Chem., Abs. B, 1933; 22: 453-464.

[41]. Kim E.C. and Kang S.G. Solid State Commun.1996; 97: 991-995.

[42]. Hsu F-C, Luo J-Y, Yeh K-W, Chen T-K, Huang T-W, Wu P.M., Lee Y-C, Huang Y-L, Chu Y-Y, Yan D-C and Wu M-K. Proc. Natl Acad. Sci 2008; 105: 14262.

[43]. C. Kittel, Introduction to Solid State Physics (4th ed.), page 465 ISBN 0-471-49021-0.